

Predictions of molecular chirality and helical twisting powers: A theoretical study

David J. Earl and Mark R. Wilson^{a)}

Department of Chemistry, University of Durham, South Road, Durham, DH1 3LE, United Kingdom

(Received 12 June 2003; accepted 19 August 2003)

A theoretical study of a number of chiral molecules has been undertaken using a molecular Monte Carlo simulation approach coupled with calculations of molecular chirality based on a chirality order parameter. Results for a variety of TADDOL ($\alpha, \alpha, \alpha', \alpha'$ -tetraaryl-1,3-dioxolan-4,5-dimethanol) derivatives show good agreement with experimental findings for the sign, magnitude, and the temperature dependence of the helical twisting power (HTP). For a photochromic chiral dopant with variable HTP we are able to model the reduction in the HTP when photoisomerization occurs. Our studies on a liquid crystalline material with a single chiral center have reproduced a temperature dependent twist inversion in the material. We discuss the temperature and solvent dependence of the helical twisting power and argue that in all the systems studied here, preferential selection of certain molecular conformations at different temperatures and in different solvents are able to explain the observed experimental behavior of the HTP. © 2003 American Institute of Physics. [DOI: 10.1063/1.1617980]

I. INTRODUCTION

When chiral molecules are added to an achiral liquid crystal mesophase, they can transmit their chirality to the whole system over distances many times their molecular length, giving the liquid crystal a right-handed or left-handed (depending on the enantiomer added) helical twist. Moreover, different chiral molecules can induce different levels of twist. The helical twisting power (HTP), β_M , of a chiral dopant is defined as

$$\beta_M = (Pc_w r)^{-1}, \quad (1)$$

where P is the helical pitch of the resultant phase ($P = 2\pi/k$), c_w is the weight concentration of chiral dopant and r is the enantiomeric purity of the dopant. Chiral molecules with very high HTPs ($> 100 \mu\text{m}^{-1}$) are of great industrial importance. They can be used in liquid crystal displays and in chiral polymer films to improve viewing angles in display applications.¹⁻³ In each case it is essential that a high degree of twist is imparted from just a small amount of chiral dopant, so as not to perturb other material properties, and, in some cases, because the dopant is sparingly soluble in the liquid crystal host. The production of new chiral dopant molecules can be a long and costly process, and the HTP of the molecule is unknown until it can be determined by experiment after it has been synthesized and purified. Clearly theoretical tools for predicting HTPs would be useful in determining future synthetic target molecules, and would greatly aid in the understanding of how chirality is transferred from the molecular level to the mesoscopic level.

A chiral molecule is defined as having no mirror symmetry, i.e., the mirror image of the molecule is nonsuperim-

posable upon the original. An actual quantitative measure of the magnitude of chirality for a given molecular conformation and a link to pseudoscalar properties such as the HTP or circular dichroism, has been more difficult to obtain. However, recent success has been found through calculations of the difference in chemical potential for enantiomers in a twisted nematic host,^{4,5} in calculations of a scaled chiral index,^{6,7} using a mean field approximation that takes into account chiral dispersive interactions⁸ and with the chirality order parameter approach of Nordio, Ferrarini, and co-workers.⁹⁻¹⁶ In order to determine a relationship between the molecular shape and a pseudoscalar property such as the HTP, these studies have, by necessity, been limited to relatively rigid chiral dopants where the molecular conformation is unlikely to vary significantly from the minimum energy structure that can be found from x-ray diffraction experiment and by theoretical techniques such as molecular mechanics and density functional theory. However, many important chiral dopants have a much higher degree of molecular flexibility.

In this paper we have combined the chirality order parameter approach of Nordio *et al.*⁹⁻¹⁶ with Monte Carlo simulations to study a range of systems. The simulation approach used is described in Sec. II, and results are presented in Secs. III and IV for a series of binaphthol and helicene chiral dopant compounds, TADDOL derivatives, a chiral photochromic dopant with variable HTP, a liquid crystalline material that undergoes a temperature induced twist inversion in the cholesteric phase, and a series of achiral banana molecules that have been found to act as chiral dopants when added to a cholesteric liquid crystal. Finally, in Sec. V we draw some conclusions as to the strengths and weaknesses of the method, and discuss possible extensions to the work presented here.

^{a)} Author to whom correspondence should be addressed.
Tel: +44 191 334 2144; Fax: +44 191 386 1127;
electronic mail: mark.wilson@durham.ac.uk

II. COMPUTATIONAL METHOD

In the surface chirality model developed by Nordio, Ferrarini, and co-workers^{9–16} the helical twisting power, β_M , at a temperature T , is obtained from

$$\beta_M = \frac{RT\varepsilon\chi}{2\pi K_{22}\nu_m}, \quad (2)$$

where ε , ν_m , and K_{22} are, respectively, the strength of the orienting potential, the molar volume of the nematic solution, and the twist elastic constant of the solvent. The quantity χ is defined as the chirality order parameter and describes the coupling between the chiral surface of the molecule and its orientational ordering. Positive values of χ lead to a right-handed twisted nematic being induced in the liquid crystal host. The theory is based upon the assumption that the alignment of a solute molecule in a locally nematic environment can be determined purely from the molecular shape of the solute, and that the chiral shape of a molecule is able to exert a torque on the local nematic director over distances many times its molecular length due to the elastic properties of the nematic phase.

χ can be obtained for any molecule from a calculation of 3 tensors, the surface tensor, \mathbf{T} , the helicity tensor, \mathbf{Q} , and the ordering matrix, \mathbf{S} . The theory has been described in detail elsewhere^{10,15,16} so we include only a brief summary of the technique as applied to the molecules studied here. We define initially a molecular surface using the Simple Invariant Molecular Surface (SIMS) method of Vorobjev and Hermans,¹⁷ which generates a surface from a rolling sphere algorithm. Here we employ a point density of 10 \AA^{-2} and a probe radius of 2.5 \AA for the rolling sphere. In tests, the latter was found to give the best agreement with calculated values of β_M for a series of rigid molecules with known HTPs (see Sec. III). Numerical integration over surface points (typically >2000 points per molecule) yielded the surface tensor

$$T_{ij} = \frac{-3 \int_S s_i s_j dS + S \delta_{ij}}{\sqrt{6}}, \quad (3)$$

where δ_{ij} is the Kronecker delta and \mathbf{s} is a unit vector along the outer normal of the molecular surface element dS . Diagonalization of \mathbf{T} yielded the components (T_{xx} , T_{yy} , T_{zz}) that define the tendency of the molecular principal axes to align parallel (T_{zz}) and perpendicular (T_{xx} , T_{yy}) to the nematic director. Numerical integration over the molecular surface also yields the helicity tensor

$$Q_{ij} = -\left(\frac{3}{8}\right)^{1/2} \sum_{k,l} \int_S [r_k s_l (\varepsilon_{ikl} s_j + \varepsilon_{jkl} s_i)] dS, \quad (4)$$

where ε_{ijk} is the Levi-Civita symbol and \mathbf{r} is a vector from the origin of the molecular axis to a surface element dS . The helicity center, r^H , was calculated from \mathbf{Q} (see Ref. 10), and the helicity tensor recalculated using r^H as the origin in Eq. (4). Finally, \mathbf{Q} was obtained in the principal axis system of the \mathbf{T} tensor and the diagonal components (Q_{xx} , Q_{yy} , Q_{zz}) were used in the calculation of χ .

The orientational behavior of the solute molecule within the liquid crystal phase was calculated by defining an orienting potential

$$\frac{U(\Omega)}{k_B T} = \varepsilon \int_S P_2(\mathbf{n} \cdot \mathbf{s}) dS, \quad (5)$$

where $U(\Omega)$ is the orienting potential at the molecular orientation Ω , P_2 is the second Legendre polynomial, and \mathbf{n} is the nematic director (taken along the Z-axis). Equation (5) is analogous to the surface anchoring potential which has been used to determine the orientations of liquid crystal molecules in bulk nematics.^{18–21} The Cartesian components of the ordering matrix \mathbf{S} can be obtained by calculating

$$S_{ij} = \int \frac{(3l_{zi}l_{zj} - \delta_{ij})}{2} P(\Omega) d\Omega, \quad (6)$$

where l_{zi} is the cosine of the angle between the Z laboratory axis and the i molecular axis and $P(\Omega)$ is the orientational distribution function defined by

$$P(\Omega) = \frac{\exp[-U(\Omega)/k_B T]}{\int \exp[-U(\Omega)/k_B T] d\Omega}. \quad (7)$$

To evaluate $P(\Omega)$ [Eq. (7)], and hence \mathbf{S} , we performed a double integration over the β and γ Euler angles using 1000 points for each angle.²² Finally, the chirality order parameter was obtained as

$$\chi = -\left(\frac{2}{3}\right)^{1/2} (Q_{xx}S_{xx} + Q_{yy}S_{yy} + Q_{zz}S_{zz}), \quad (8)$$

where the components S_{ii} are obtained by expressing \mathbf{S} in the principal axis system of the surface tensor \mathbf{T} .

Equations (2)–(8) are given for a single conformation. However, Eq. (2) is equally valid for an average χ obtained from a statistically significant and independent number of conformations of a molecule. To take into account the conformational dependence of χ we used an internal coordinate Monte Carlo (MC) technique, where molecules were represented by a Z-matrix. We used an augmented form of the MM2 (Ref. 23) force field, taken from an initial energy minimization using the CACHE program.²⁴ Full details of our MC technique are described in Ref. 25. Sampling of χ was carried out at intervals of 200 MC steps with a new molecular surface generated for each sample. For each molecule and each temperature studied, runs in excess of 2×10^6 MC steps were carried out. Checks for convergence of the mean steric energy, χ values, and of dihedral angle distributions were carried out in each case. In most cases convergence of averages occurred within 5×10^5 MC steps.

III. RIGID CHIRAL MOLECULES

To verify that χ from Sec. II was applicable to complex chiral molecules, we studied a series of rigid molecules: bridged biaryl²⁶ and helicene derivatives^{12,27} (Fig. 1). These are molecules where one particular molecular conformation dominates and their experimental helical twisting powers show little temperature dependence. For these reasons, they are an excellent choice to test the theoretical methods used here and will provide a good comparison with experimental results.

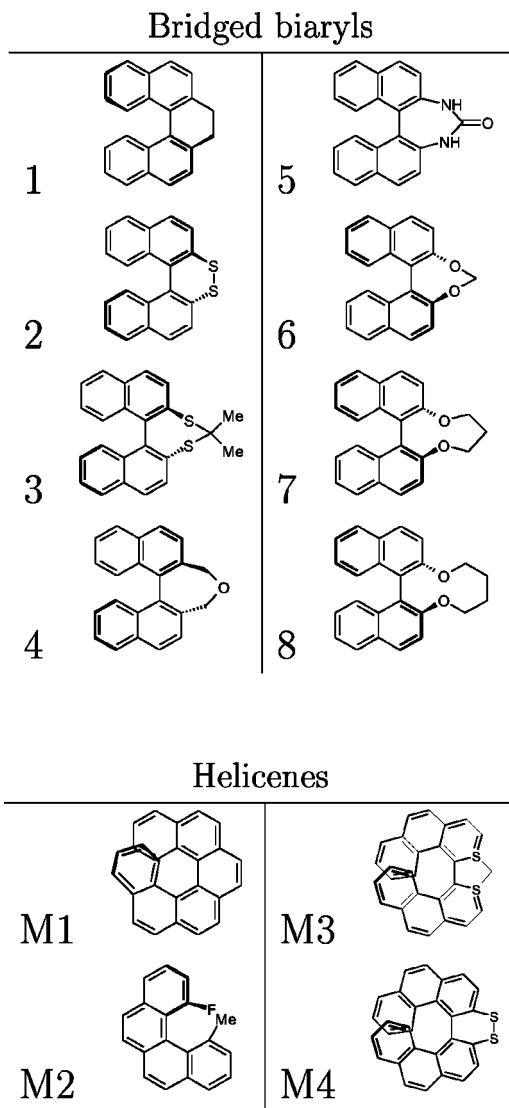


FIG. 1. Structures of the bridged biaryl (1–8) and helicene derivatives (M1–M4) studied.

For each of the molecules in Fig. 1, the optimized geometry was determined using an augmented MM3 force-field.²⁸ The chirality order parameter was then calculated for each of these molecular structures using the method described in Sec. II and the results are shown in Table I.

TABLE I. Diagonal components of the helicity tensor \mathbf{Q} , and the ordering matrix \mathbf{S} , chirality order parameter χ , and the experimental helical twisting powers β_M , taken from Refs. 26, 27 for the bridged biaryl and helicene molecules in Fig. 1. Values of χ from Ref. 12 using a probe radius of 0 Å are included in brackets for comparison for molecules M1–M4.

Molecule	Q_{xx}	Q_{yy}	Q_{zz}	S_{xx}	S_{yy}	S_{zz}	$\chi/\text{Å}^3$	$\beta_M/\mu\text{m}^{-1}$
1	-103	79	24	0.05	-0.37	0.31	+21.9	+69
2	90	-67	-23	0.06	-0.38	0.31	-19.2	-65
3	24	-85	62	0.03	-0.33	0.31	-39.1	-71
4	125	-101	25	-0.02	-0.32	0.35	-17.1	-55
5	92	-63	-29	0.12	-0.38	0.26	-22.4	-21
6	-116	92	25	0.02	-0.35	0.33	+21.6	+85
7	-137	93	45	0.06	-0.31	0.26	+21.0	+80
8	-124	67	57	0.14	-0.33	0.19	+23.4	+79
M1	69	-68	-1	0.04	-0.39	0.36	-23.6 (-36)	-55
M2	61	-44	-17	-0.04	-0.37	0.40	-5.8 (-12)	-9
M3	37	-55	18	0.05	-0.39	0.34	-23.8 (-43)	-20
M4	41	-50	9	-0.01	-0.39	0.40	-18.2 (-25)	-13

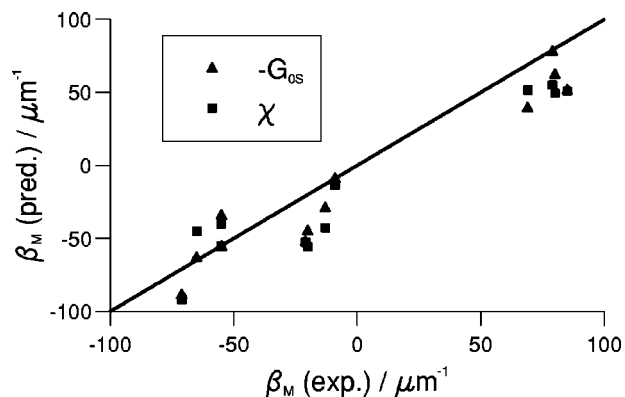


FIG. 2. The predicted HTP for the bridged biaryl and helicene derivative molecules use the chirality order parameter (squares), χ [as defined in Eq. (8)], and the scaled chiral index (triangles), $-G_{0S}$ [as defined in Eq. (10)], compared to the experimental HTP.

To calculate predicted values of β_M in Fig. 2 a scaling factor was used. In our model T , ϵ , and K_{22} are unchanged for all dopants and at low dopant concentrations ν_m tends towards the molar volume of the solvent, so we determine a predicted β_M as

$$\beta_M = D\chi, \quad (9)$$

where D is a constant found from a best fit to the experimental data.^{26,27} Here we use a value of $D = 2.351 \text{ Å}^{-3} \mu\text{m}^{-1}$.

The results in Fig. 2 show good agreement with experimental findings. The sign of β_M is correctly predicted in each case, and the magnitude of β_M is predicted with an average error of $\pm 22 \mu\text{m}^{-1}$. Coupled with the rapid calculation time for χ this makes the chirality order parameter a useful tool for the study of more complex flexible molecules, where a large number of molecular conformations are likely to contribute to the overall HTP observed in experiments. Ferrarini *et al.*¹² have also studied helicene molecules M1 \rightarrow M4. Our results differ slightly from those in the previous work due to the size of the probe radius used to generate the molecular surface. We note that when we consider the molecules as an assembly of van der Waals spheres (probe radius of 0 Å) we obtain results that are very similar to those in the Ferrarini *et al.* study.

As a comparison in Fig. 2 we show also predicted values of β_M determined using the scaled chiral index^{6,7,29} that is calculated from

$$G_{0S} = \frac{1}{3} \frac{4!}{N^4} \left[\sum_{i,j,k,l=1}^N \omega_i \omega_j \omega_k \omega_l \times \frac{[(\mathbf{r}_{ij} \times \mathbf{r}_{kl}) \cdot \mathbf{r}_{il}](\mathbf{r}_{ij} \cdot \mathbf{r}_{jk})(\mathbf{r}_{jk} \cdot \mathbf{r}_{kl})}{(r_{ij} r_{jk} r_{kl})^n r_{il}^m} \right], \quad (10)$$

where the sum includes the contribution of all permutations of four points (atoms), \mathbf{r}_i is the position of atom i , $\mathbf{r}_{ij} = \mathbf{r}_i - \mathbf{r}_j$, N is the number of atoms and the weighting factors $\omega_{i,j,k,l}$ can be a physical quantity associated with the point/atom. We will consider the case where $n=2$ and $m=1$, corresponding to a dimensionless index and we set $\omega_{i,j,k,l}=1$, although alternatively it could be set to any representative physical quantity to give extra weight to certain points. In Fig. 2 we determine a predicted β_M for G_{0S} as

$$\beta_M = -JG_{0S}, \quad (11)$$

where J is a constant found from a best fit to experimental data. Here we use a value of $J=0.523 \mu\text{m}^{-1}$. As reported recently,³⁰ we find a similar level of agreement between the G_{0S} and χ methods (average error for $G_{0S} \pm 17 \mu\text{m}^{-1}$). However, the chirality order parameter is an order of magnitude less expensive to calculate for the systems studied and increases with the approximate square of the number of atoms, N , as opposed to N^4 for G_{0S} . The former is therefore better suited for the thousands of individual calculations required in a full Monte Carlo study of a flexible molecule.

IV. FLEXIBLE CHIRAL MOLECULES

A. TADDOL derivatives

The TADDOL family of molecules are based on the structural core shown in Fig. 3(a). TADDOL derivatives have a wide variety of HTPs ranging from around $20 \mu\text{m}^{-1}$ to an extraordinarily large $300 \mu\text{m}^{-1}$ and are relatively soluble in polar solvents making them good candidates for use as chiral dopants.³¹ They exhibit a high degree of flexibility around torsional angles ϕ_{1-8} [shown in Fig. 3(a)] giving them considerable conformational freedom. Three TADDOL derivatives were studied with widely different HTPs [Fig. 3(b)]. The simulations were carried out at three temperatures between 300 K and 350 K for each of the molecules using the MC approach described in Sec. II. In addition we carried out an initial test calculation of an achiral molecule, hexane, which yielded $\langle \chi \rangle = (-0.00017 \pm 0.00619) \text{ \AA}^3$.

Following Ferrarini *et al.*³² we approximate the ordering strength parameter, ε , to vary as $1/k_B T$ and we set $\varepsilon = 0.05 \text{ \AA}^{-2}$ at $T=300 \text{ K}$. Results are presented in Fig. 4 with the simulation value of β_M determined as in Sec. III using $D=2.351 \text{ \AA}^{-3} \mu\text{m}^{-1}$. For comparison we also present results for the case where $\varepsilon=0.05 \text{ \AA}^{-2}$ at all temperatures. The magnitude of the HTP in Fig. 4 is predicted to a good accuracy and the trend of decreasing HTP with increasing temperature is also observed, although the effect is not as pronounced in the simulation. For TADDOLs A and B,

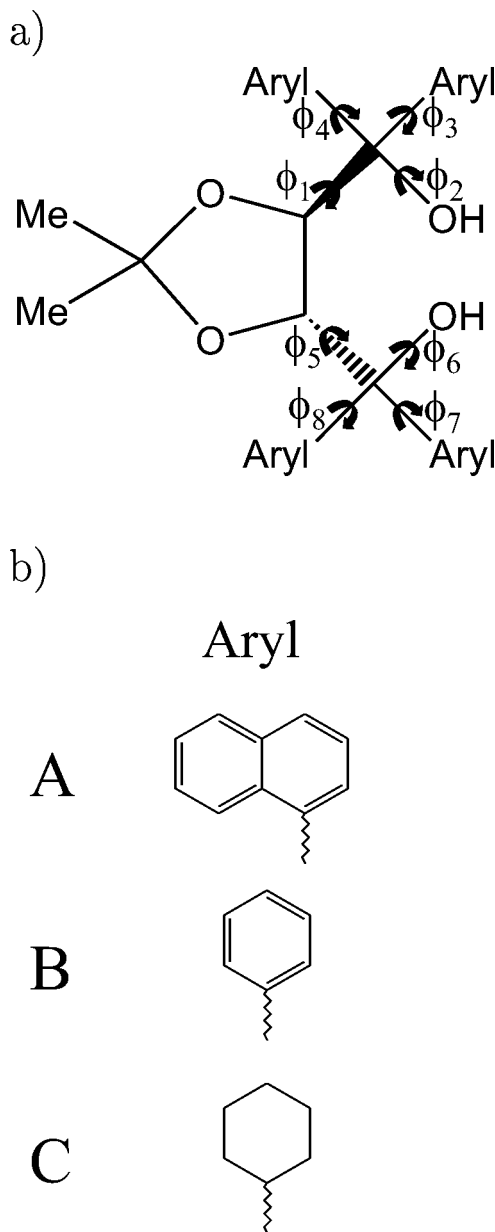


FIG. 3. (a) Basic TADDOL structure showing the flexibility around dihedral angles $\phi_1 \rightarrow \phi_8$. (b) TADDOL derivatives A, B, C, where the structures shown are the Aryl substituents in (a).

the drop in HTP can partly be attributed to the decrease in ε with temperature, but another effect comes from conformational changes (see below).

It is important to realize that the technique we use samples molecular conformations in the gas phase, and not in the liquid crystal phase where solute-solvent interactions are likely to influence the relative weight of different conformations.^{33,34} However, we can use the model to determine what conformations give rise to particularly high chirality order parameters (and hence HTPs) and also examine how a change in temperature influences the selection of these conformations. Figure 5(a) shows how the chirality order parameter varies with the dihedral angle ϕ_8 for structure B at 350 K. (Noting that the behavior of ϕ_8 is identical to that of ϕ_4 .) For ϕ_8 (and ϕ_4) the chirality order parameter varies as a cosine wave with a period of π . We observe

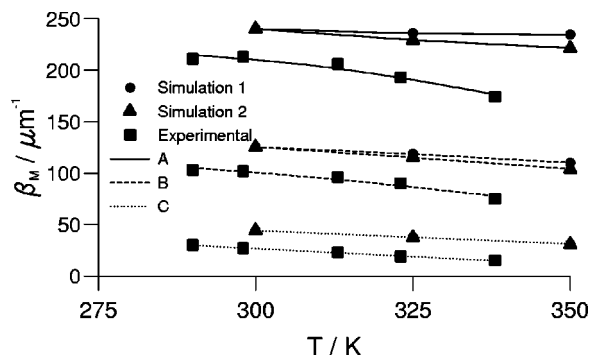


FIG. 4. Predicted HTPs from simulation results with a constant ordering strength (1) (circles) and with an ordering strength with a $1/k_B T$ dependence (2) (triangles) as a function of temperature compared to experimental findings (squares) from Ref. 31 for TADDOL derivatives A (solid line), B (dashed line), and C (dotted line).

conformations with high chirality at $\sim 0^\circ$ (α conformations, $315^\circ \rightarrow 45^\circ$) and $\sim 180^\circ$ (γ conformations, $135^\circ \rightarrow 225^\circ$) and low chirality at $\sim 90^\circ$ (β conformations, $45^\circ \rightarrow 135^\circ$) and $\sim 270^\circ$ (δ conformations, $225^\circ \rightarrow 315^\circ$). If conformations α and γ are preferentially selected at lower temperatures compared to β and δ , then this would explain the temperature dependence observed in the simulation and potentially in the

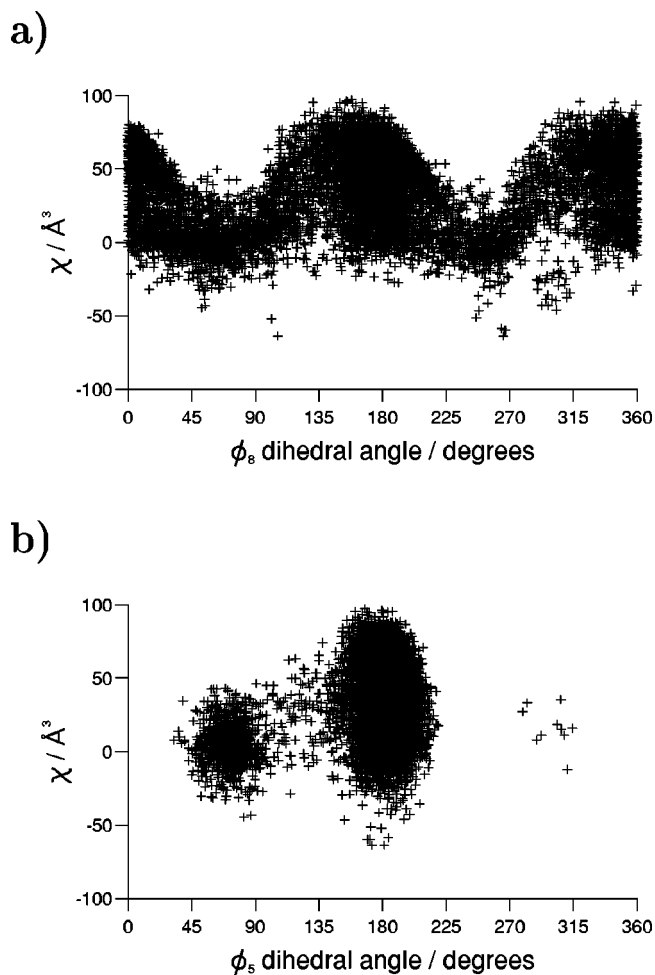


FIG. 5. Variation of chirality order parameter for structure B at 350 K with (a) dihedral angle ϕ_8 and (b) dihedral angle ϕ_5 .

TABLE II. Relative populations of low and high chirality conformations for structure B.

T/K	ϕ_8 dihedral angle population/%					
	α	β	γ	δ	$\alpha + \gamma$	$\beta + \delta$
300	43.5	4.5	44.8	7.2	88.2	11.8
325	34.5	9.0	45.6	10.9	80.1	19.9
350	33.8	10.9	43.5	11.8	77.3	22.7

experimental system. Table II shows the relative populations of α , β , γ , and δ conformations for structure B between 300 K and 350 K. Table II clearly shows a trend of decreasing populations of high chirality conformations and increasing populations of low chirality conformations as the temperature decreases. As the temperature increases eventually all conformations will become equivalent. However, it is of interest that high chirality conformations in these TADDOL derivatives dominate in the temperature regime of typical nematic liquid crystalline materials.

Dihedral angles ϕ_1 and ϕ_5 are also of interest. The variation of the chirality order parameter with rotation about ϕ_5 for structure B at 350 K can be seen in Fig. 5(b). For conformations with ϕ_5 and $\phi_1 \approx 180^\circ$ intramolecular hydrogen bonding will occur. For other conformations ($\sim 60^\circ$ and $\sim 300^\circ$) intramolecular hydrogen bonding is not possible. Figure 5(b) demonstrates that structures with intramolecular hydrogen bonding generally have greater values of χ than nonhydrogen bonding conformations. For the nonhydrogen bonding conformations of structure B, $\langle \chi \rangle \approx 6 \text{ \AA}^3$, whereas for hydrogen bonding conformations $\langle \chi \rangle \approx 55 \text{ \AA}^3$. In our simulations we also see a trend of increasing nonhydrogen bonding conformations as the temperature increases. For example, for structure B at 300 K 95.9% of structures are intramolecular hydrogen bonding conformations, compared to 93.4% at 325 K and 90.4% at 350 K. In experimental systems the preference of selection of hydrogen bonding conformations in different solvents (for example, the preferential selection of these conformations in organic nonpolar solvents) is expected to have a large impact on the observed HTPs of these systems.

In the experimental system it is likely that the decrease in molecular order of the solvent with temperature will also lead to a decrease in ϵ , as ϵ is predicted to be proportional to the order parameter.³² Together with the solvent effect on conformation, this is likely to contribute most to the difference between experimental and predicted values.

B. Chiral photochromic molecule with variable helical twisting power

In a recent experimental paper by Bobrovsky *et al.*³⁵ detailed work was conducted on a photosensitive chiral dopant (Fig. 6). The synthesized dopant molecule was found to have an experimental HTP of $\beta_M \approx 45 \mu\text{m}^{-1}$. However, upon exposure to ultraviolet (UV) light the HTP of the dopant was found to decrease significantly. Here photoisomerization will occur around a C=C bond forming the Z-E isomer, which can further photoisomerize around the other C=C bond to give the Z-Z isomer (see Fig. 6). The experimental paper

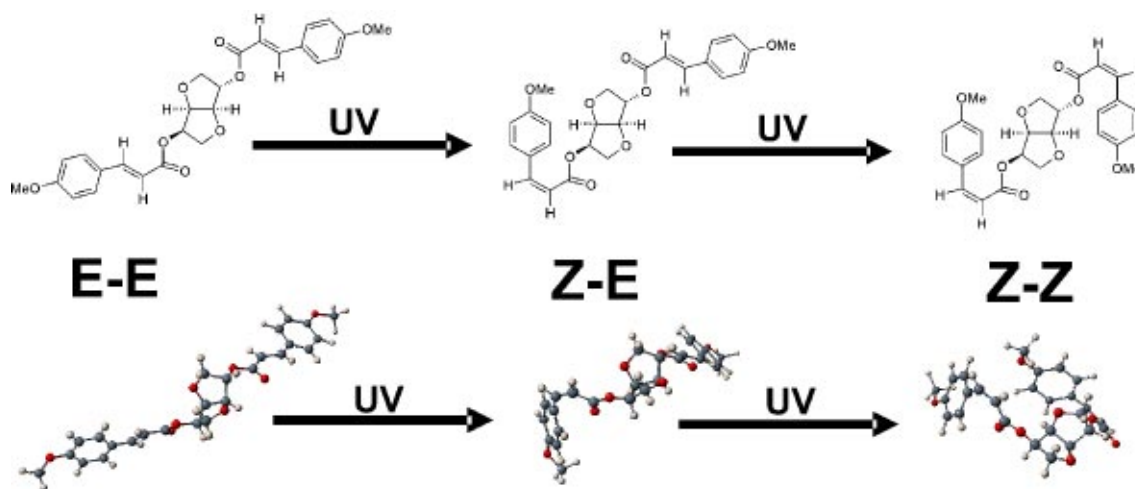


FIG. 6. Photoisomerization of an isosorbide chiral dopant when exposed to UV light. (Top) Structures of isomers. (Bottom) Snapshots from simulation.

does not quote the percentages of each isomer present, but an accurate theoretical study should be able to predict a drop in the HTP as the E–E isomer is photoisomerized.

Gas phase, flexible molecular Monte Carlo simulations were performed on the E–E, the Z–E, and the Z–Z isomers at 400 K. The relatively high temperature ensures excellent conformational sampling, and we note that the calculated value of $\langle\chi\rangle$ does not vary significantly with temperature for these structures. An orienting strength parameter $\varepsilon = 0.05 \text{ \AA}^{-2}$ was used to determine the expected HTPs of each of these structures using 10 000 conformations from the simulations to calculate an average chirality order parameter, χ , for each of the structures. For the E–E isomer $\langle\chi\rangle = 49.7 \pm 1.6 \text{ \AA}^3$. Upon photoisomerization the chirality drops significantly; for the Z–E photoisomer $\langle\chi\rangle = 8.0 \pm 0.9 \text{ \AA}^3$, and for the Z–Z photoisomer $\langle\chi\rangle = 13.8 \pm 0.9 \text{ \AA}^3$. The results demonstrate that the E–E isomer is theoretically predicted to have a much higher chirality order parameter, and hence HTP, than the Z–E and the Z–Z isomers and therefore explains the drop in HTP upon exposure to UV light.

C. Temperature dependent twist inversion molecule

In 1992, Goodby *et al.*³⁶ published experimental findings on the liquid crystalline material S-2-chloropropyl 4'-(4''-n-nonyloxyphenylpropionyloxy)biphenyl-4-carboxylate which contains a single chiral center and whose structure is shown in Fig. 7. Their results were surprising and demonstrated that the material underwent an inversion of the helical

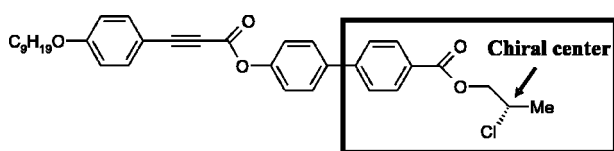


FIG. 7. Structure of S-2-chloropropyl 4'-(4''-n-nonyloxyphenylpropionyloxy)biphenyl-4-carboxylate showing the single chiral center of the molecule. The boxed structure indicates the fragment molecule used in the *ab initio* calculations of Sec. IV C (a single hydrogen atom was added to the phenyl ring of this structure to complete valence).

twist sense in the chiral nematic phase from a left-handed twist at lower temperatures to a right-handed twist at higher temperatures. They suggested that the helix inverts due to changes in the populations of conformational isomers at different temperatures. However, they were unable to determine the twist senses of individual conformations to confirm their theory for the origin of the twist mechanism.³⁷ Here we apply our Monte Carlo technique to the material and attempt to recreate the temperature dependence of the twist-sense and to explain why it occurs.

An initial investigation into the O–C–C–Cl dihedral angle, around the chiral center of the molecule, was required as it is known that the MM2 force field does not model dihedral angles of this type correctly. The dihedral angle energy was calculated using density functional theory (DFT) at the B3LYP/6-31G* level for the fragment molecule shown in Fig. 7 and the results are depicted in Fig. 8. The torsional angle was studied at intervals of 15° and geometry optimization was carried out at all points. A further geometry optimization was conducted in each of the three potential wells to ensure the energies of the minima were calculated correctly. The conformation with the Cl atom *trans* to the core of the molecule (*T*) was found to be the most stable, fol-

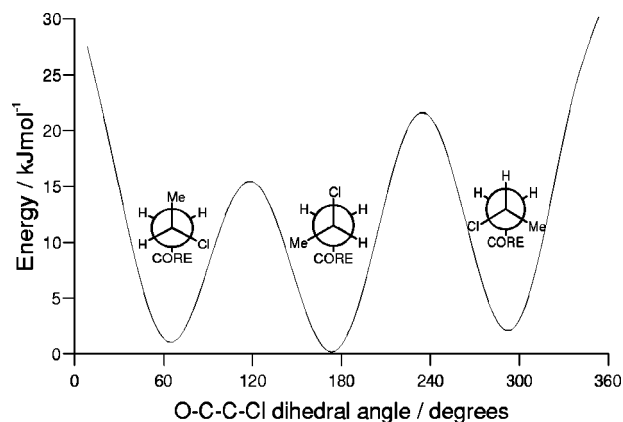


FIG. 8. Calculated torsional energies for the O–C–C–Cl dihedral angle from DFT calculations.

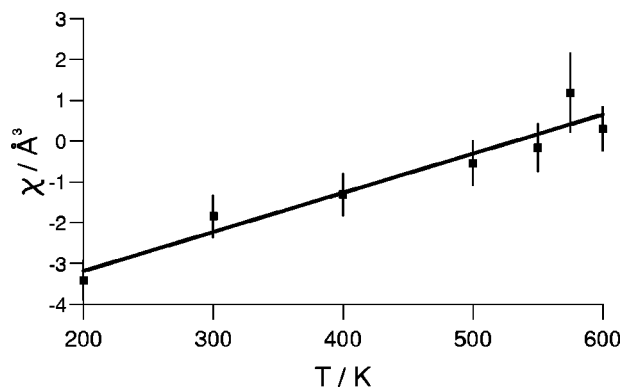


FIG. 9. The chirality order parameter, χ , as a function of temperature for S-2-chloropropyl 4'-(4''-n-nonyloxyphenylpropioiloxy)biphenyl-4-carboxylate.

lowed by the Me group *trans* to the core ($G-$), with the H atom *trans* to the core ($G+$) being the minimum with the highest energy conformations and thus the least favored of the three potential minima. Our calculations differ significantly from those of Goodby *et al.*³⁷ who found that the H *trans* conformation was more stable than the Me *trans* conformation. However, the latter was carried out using the cruder force field representation within the program CHARMM.^{38,39}

Using the DFT data the MM2 force field was augmented to reproduce the dihedral angle energy for the O–C–C–Cl dihedral. To do this we followed the dihedral fitting procedure of Cheung *et al.*,⁴⁰ to fit to the torsional terms in the force field. Gas phase, flexible molecular Monte Carlo simulations were then carried out on the molecule at a number of temperatures, and the average chirality order parameter was calculated, along with its standard error, from 10 000 conformations from the simulation. In these simulations we kept the orienting strength, ϵ , constant and set its value to 0.05 \AA^{-2} so that changes in the chirality order parameter with temperature could be studied purely as a function of changes in conformational sampling. The results are presented in Fig. 9, and show a twist inversion for the cholesteric liquid crystalline material. The simulations predict the twist inversion to occur at ~ 530 K, whereas in the experimental system the twist inversion occurs at ~ 414 K. The likely discrepancy here is caused by ignoring the influence of changes in the liquid crystalline environment on conformations and on ϵ . Despite this, prediction of a sign change in χ is impressive and suggests that the twist inversion can be explained by conformational changes.

We now turn our attention to the origin of chirality in this molecule and attempt to explain why the twist inversion occurs. A statistical analysis of data for the O–C–C–Cl dihedral at selected temperature points is shown in Table III. The relative populations of the *trans*, and two *gauche* states about the O–C–C–Cl dihedral angle are presented along with the average chirality order parameter, χ , for each of the three main states.

From these data it is possible to determine the origin of the twist inversion. At low temperatures, conformations with the O–C–C–Cl dihedral angle in the T position tend to

TABLE III. Relative populations and chirality order parameters for the three main conformations of the O–C–C–Cl dihedral angle in S-2-chloropropyl 4'-(4''-n-nonyloxyphenylpropioiloxy)biphenyl-4-carboxylate (O–C–C–Cl dihedral angles $0^\circ < G- < 120^\circ$, $120^\circ < T < 240^\circ$, $240^\circ < G+ < 360^\circ$).

T/K	Population/%			$\langle \chi \rangle / \text{\AA}^3$		
	$G-$	T	$G+$	$G-$	T	$G+$
200	18.0	75.4	6.6	7.3	-5.9	-3.9
400	27.3	59.2	13.5	6.5	-4.1	-4.9
550	30.6	53.6	15.8	6.6	-3.4	-2.4
600	31.9	49.5	18.6	5.4	-2.3	-1.4

dominate. As these conformations have a net negative chirality associated with them then the overall twist sense of the system is negative. At higher temperatures the population of the T position decreases and those of the $G-$ and $G+$ positions increase, as expected from the DFT results. The net chirality of the $G-$ position conformations is strongly positive and of greater magnitude than the negative contributions to chirality of the T and $G+$ conformations. Thus, as the temperature increases, the negative contribution to chirality from the T conformations decreases, the negative contribution from the $G+$ conformations increases slightly and the positive contributions from the $G-$ conformations increases strongly. Eventually this leads to a helical twist inversion from a left hand (negative χ) twist at lower temperatures to a right-hand (positive χ) twist at higher temperatures. Another trend is also apparent in Table III. The magnitude of the average chirality arising from the $G-$, T , and $G+$ conformations decreases as the temperature increases. This effect can be explained by a reduction in the order of the molecule at higher temperatures.

It is apparent from this study that the helix twist inversion can be explained by the different weighting of certain molecular formations, with their associated chiralities, at different temperatures. Emelyanenko⁴¹ and Osipov *et al.*⁴² have developed molecular theories of the helical sense inversion based upon the competition between dispersion and steric interactions in these systems and the biaxiality of molecules. We note that while the model we use here does not explicitly take into account any of these effects it is still able to account for the helical twist inversion purely on the basis of conformational change.

D. Achiral banana-shaped molecules

In a recent experimental study, Watanabe *et al.*⁴³ found that a series of achiral banana-shaped molecules with dodecyl tail groups (Fig. 10), when added to a cholesteric liquid crystal, enhanced the twisting power of the chiral nematic phase. In effect the achiral banana-shaped molecules were acting as chiral dopants. The experimental paper proposes that in a chiral nematic liquid crystal the banana-shaped molecules preferentially select chiral conformations with the same handed twist as the chiral phase, and thus enhance the twist of the cholesteric phase in the same way that a normal chiral dopant would. Here, we simulate the three molecules in Fig. 10. For these larger systems 4 million Monte Carlo

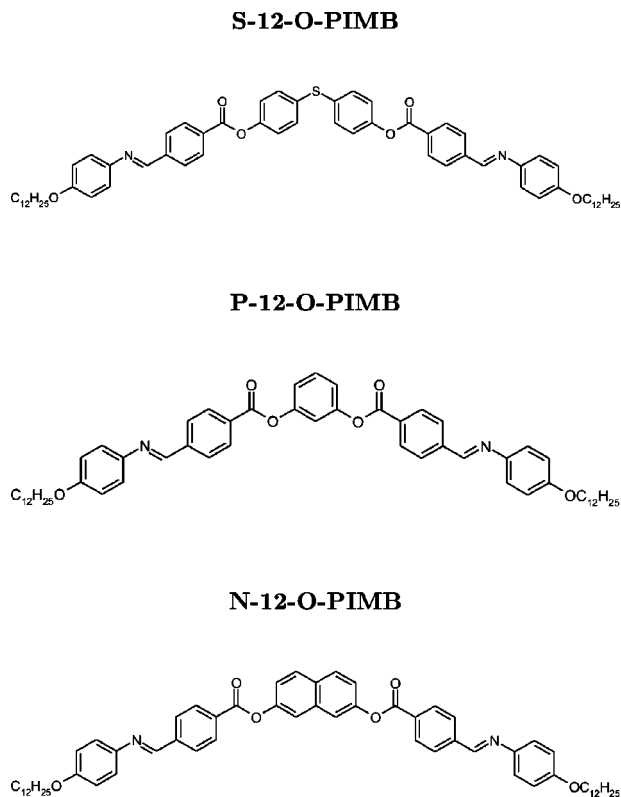


FIG. 10. Chemical structures of the three achiral banana molecules studied.

steps were required and the calculations were carried out at 400 K with an orienting strength parameter $\varepsilon = 0.05 \text{ \AA}^{-2}$. 20 000 conformations were used to determine an average chirality order parameter.

As expected, each of the molecules was found to be achiral within the statistical error of our results ($\langle \chi \rangle = 0.05 \pm 6.58 \text{ \AA}^3$ for S-12-O-PIMB, $\langle \chi \rangle = 0.25 \pm 3.93 \text{ \AA}^3$ for P-12-O-PIMB and $\langle \chi \rangle = -1.99 \pm 11.49 \text{ \AA}^3$ for N-12-O-PIMB). However, during our simulations the molecules adopted a number of conformations with extremely high magnitudes of chirality associated with them. For example, $\sim 20\%$ of the conformations adopted had $|\chi| \geq 500 \text{ \AA}^3$ and $\sim 2\%$ of the conformations had $|\chi| \geq 1000 \text{ \AA}^3$. It should be noted that χ is not a function of molecular size and that a conformation with $\chi \approx 500 \text{ \AA}^3$ corresponds to $\beta_M \approx 1000 \mu\text{m}^{-1}$, which is much higher than any helical twisting power that has been measured experimentally for chiral systems. Even a small increase in the proportion of left-handed or right-handed chiral conformations sampled by these banana-shaped molecules in the twisted nematic liquid crystal phase would have a relatively large effect on the twist of the system due to the extremely high HTPs of the chiral conformations. Thus, it seems likely in the experiments that the chiral nematic phase is preferentially selecting chiral conformations that twist in the same direction.

V. CONCLUSIONS

A flexible molecular Monte Carlo simulation approach, coupled with calculations of a chirality order parameter has been used to study a range of chiral molecules. The method has been successful in predicting helical twisting powers for

flexible chiral dopants, in predicting the temperature dependence of HTPs, and has demonstrated a temperature induced helical twist inversion. We have also shown extraordinarily high HTP values for some conformations exhibited by achiral banana molecules.

In this work we have restricted our studies to simulations of molecules in the gas phase due to the computational cheapness of this approach and the excellent conformational sampling that can be achieved. It is important to note that we would expect a liquid crystalline solvent to affect the relative weighting of conformations sampled by the molecule, and thus influence the chirality of the system. Indeed, these solute-solvent effects may account for the exaggerated temperature dependence of the HTP in the experimental system compared to our simulations for the TADDOL derivatives and may also explain differences in the predicted and experimental temperatures for helical twist inversion for S-2-chloropropyl 4'-(4''-n-nonyloxyphenylpropioyloxy)biphenyl-4-carboxylate. Our method could easily be adapted to more complicated systems where a liquid crystalline solvent (either coarse-grained^{44,45} or fully atomistic) could be included in the simulations. In these cases, we expect different conformations (with different chiralities) to be preferentially selected in different solvents, thus accounting for solvent dependent HTPs. By including a fully atomistic liquid crystal solvent it would then be possible to study the role of electrostatic and induction interactions on the helical twisting power of chiral dopants.

ACKNOWLEDGMENTS

The authors wish to thank Professor Maureen Neal and Professor John Goodby for valuable discussions. D.J.E. wishes to thank EPSRC for a studentship and Merck NB-C for an industrial CASE award.

- ¹M. C. W. van Bostel, R. H. C. Janssen, C. W. M. Bastiaansen, and D. J. Broer, *J. Appl. Phys.* **89**, 838 (2001).
- ²M. Schadt, H. Seiberle, and A. Schuster, *Nature (London)* **381**, 6579 (1996).
- ³P. van de Witte, E. E. Neuteboom, M. Brehmer, and J. Lub, *J. Appl. Phys.* **85**, 7517 (1999).
- ⁴M. J. Cook and M. R. Wilson, *J. Chem. Phys.* **112**, 1560 (2000).
- ⁵M. R. Wilson and D. J. Earl, *J. Mater. Chem.* **11**, 2672 (2001).
- ⁶M. Solymosi, R. J. Low, M. Grayson, M. P. Neal, M. R. Wilson, and D. J. Earl, *Ferroelectrics* **277**, 169 (2002).
- ⁷M. P. Neal, M. Solymosi, M. R. Wilson, and D. J. Earl, *J. Chem. Phys.* **119**, 3567 (2003).
- ⁸M. A. Osipov and H. G. Kuball, *Eur. Phys. J. E* **5**, 589 (2001).
- ⁹A. Ferrarini, G. J. Moro, and P. L. Nordio, *Liq. Cryst.* **19**, 397 (1995).
- ¹⁰L. Feltre, A. Ferrarini, F. Pacchiale, and P. L. Nordio, *Mol. Cryst. Liq. Cryst. Sci. Technol., Sect. A* **290**, 109 (1996).
- ¹¹A. di Matteo, S. M. Todd, G. Gottarelli, G. Solladie, V. E. Williams, R. P. Lemieux, A. Ferrarini, and G. P. Spada, *J. Am. Chem. Soc.* **123**, 7842 (2001).
- ¹²A. Ferrarini, G. Gottarelli, P. L. Nordio, and G. P. Spada, *J. Chem. Soc., Perkin Trans. 1* **2**, 411 (1999).
- ¹³A. Ferrarini and P. L. Nordio, *J. Chem. Soc., Perkin Trans. 1* **2**, 455 (1998).
- ¹⁴A. Ferrarini, P. L. Nordio, P. V. Shibaev, and V. P. Shibaev, *Liq. Cryst.* **24**, 219 (1998).
- ¹⁵A. Ferrarini, G. J. Moro, and P. L. Nordio, *Mol. Phys.* **87**, 485 (1996).
- ¹⁶A. Ferrarini, G. J. Moro, and P. L. Nordio, *Phys. Rev. E* **53**, 681 (1996).
- ¹⁷Y. Vorobjev and J. Hermans, *Biophys. J.* **73**, 722 (1997).
- ¹⁸A. Rapini and M. Papoular, *J. Phys. Colloq.* **30 C4**, 54 (1969).

- ¹⁹P. G. de Gennes, *The Physics of Liquid Crystals* (Oxford University Press, Oxford, 1974), Chap. 3.
- ²⁰F. Brochard and P. G. de Gennes, *J. Phys. (Paris)* **31**, 691 (1970).
- ²¹S. V. Burylov and Y. L. Raikher, *Phys. Lett. A* **149**, 279 (1990).
- ²²A. Ferrarini (personal communication, 2002).
- ²³N. L. Allinger, *J. Am. Chem. Soc.* **99**, 8127 (1977).
- ²⁴*CACHE Satellite: A Chemists Guide to CACHE for Windows* (Oxford Molecular Group Inc., 1995).
- ²⁵M. R. Wilson, *Liq. Cryst.* **21**, 437 (1996).
- ²⁶G. Gottarelli, M. Hibert, B. Samori, G. Solladie, G. P. Spada, and R. Zimmermann, *J. Am. Chem. Soc.* **105**, 7318 (1983).
- ²⁷G. Gottarelli, G. Proni, G. P. Spada, D. Fabbri, S. Gladioli, and C. Rosini, *J. Org. Chem.* **61**, 2013 (1996).
- ²⁸N. L. Allinger, Y. H. Yuh, and J. Lii, *J. Am. Chem. Soc.* **111**, 8551 (1989).
- ²⁹M. Solymosi, R. J. Low, M. Grayson, and M. P. Neal, *J. Chem. Phys.* **116**, 9875 (2002).
- ³⁰H. Kamberaj, M. A. Osipov, R. J. Low, and M. P. Neal (unpublished).
- ³¹H. G. Kuball, B. Weiss, A. K. Beck, and D. Seebach, *Helv. Chim. Acta* **80**, 2507 (1997).
- ³²A. Ferrarini, G. R. Luckhurst, P. L. Nordio, and S. J. Roskilly, *Liq. Cryst.* **21**, 373 (1996).
- ³³C. McBride, M. R. Wilson, and J. A. K. Howard, *Mol. Phys.* **93**, 955 (1998).
- ³⁴M. R. Wilson and M. P. Allen, *Mol. Cryst. Liq. Cryst.* **198**, 465 (1991).
- ³⁵A. Y. Bobrovsky, N. I. Boiko, and V. P. Shibaev, *Mol. Cryst. Liq. Cryst.* **363**, 35 (2001).
- ³⁶A. J. Slaney, I. Nishiyama, P. Styring, and J. W. Goodby, *J. Mater. Chem.* **2**, 805 (1992).
- ³⁷M. J. Watson, M. K. Horsburgh, J. W. Goodby, K. Takatoh, A. J. Slaney, J. S. Patel, and P. Styring, *J. Mater. Chem.* **8**, 1963 (1998).
- ³⁸M. K. B. R. Gelin, *Biochemistry* **18**, 1256 (1979).
- ³⁹B. R. Brooks, R. E. Brucoleri, B. D. Olafson, D. J. States, S. Swaminathan, and M. Karplus, *J. Comput. Chem.* **4**, 187 (1983).
- ⁴⁰D. L. Cheung, S. J. Clark, and M. R. Wilson, *Phys. Rev. E* **65**, 051709 (2002).
- ⁴¹A. V. Emelyanenko, *Phys. Rev. E* **67**, 031704 (2003).
- ⁴²A. V. Emelyanenko, M. A. Osipov, and D. A. Dunmur, *Phys. Rev. E* **62**, 2340 (2000).
- ⁴³J. Thisayukta, H. Niwano, H. Takezoe, and J. Watanabe, *J. Am. Chem. Soc.* **124**, 3354 (2002).
- ⁴⁴J. G. Gay and B. J. Berne, *J. Chem. Phys.* **74**, 3316 (1981).
- ⁴⁵D. J. Earl, J. Ilnytskyi, and M. R. Wilson, *Mol. Phys.* **99**, 1719 (2001).